

# Model-Based Automated Functional Testing—Methodology and Application to Air-Handling Units

**Peng Xu, PhD, PE**  
Member ASHRAE

**Philip Haves, PhD**  
Fellow ASHRAE

**Moosung Kim**

## ABSTRACT

*The paper describes a model-based approach to automated functional testing at the component level and presents results from preliminary field testing of a prototype software tool that implements the method. The method is based on an integrated life-cycle approach to HVAC commissioning and performance monitoring. The tool uses component-level HVAC equipment models implemented in an equation-based simulation environment. When used for commissioning, each model is configured using design information and component manufacturers' data. Once an acceptable functional test has been performed, the model is fine-tuned to match the actual performance of the equipment by using data measured during the functional test. The fine-tuned model is then used in routine operation for on-line monitoring and fault detection. The paper describes the method and reports test results from HVAC secondary systems in a commercial building and an experimental facility.*

## INTRODUCTION

There is a growing interest in developing automated functional test methods for building HVAC systems. Functional tests can detect operation faults in HVAC systems and so save energy, reduce maintenance costs, and improve comfort. Various functional test guidelines and libraries of procedures have been developed over the last few years to promote the practice of commissioning (Sellars et al. 2003). However, currently, functional tests are mostly conducted manually by commissioning agents, which is relatively costly and does not take full advantage of the capabilities of energy management and control system (EMCS). This indicates a need for an automated functional tests tool that can be embedded in, or coupled

to, the EMCS to conduct the tests automatically. Automated functional testing has a number of potential advantages over conventional manual testing. It is expected to be easier to perform and more cost-effective, and it can be performed more frequently to detect faults earlier. In addition, the format of the data generated by automated tests is easier to standardize for data analysis.

One approach to automating both commissioning and performance monitoring is to use computer-based methods for fault detection and diagnosis (FDD). Component-level FDD, which is the basis of the approach presented here, uses a bottom up methodology to detect individual faults by analyzing the performance of each component in the HVAC system (Hyvärinen and Kärki 1997; LBNL 1999; Haves and Khalsa 2000; Ngo and Dexter 1998). In this study, an automated fault detection tool has been developed, based on an integrated life-cycle approach to commissioning and performance monitoring. The tool uses component-level HVAC equipment models implemented in the SPARK equation-based simulation environment (SPARK 2004). When used for commissioning, each model is configured using design information and component manufacturers' data. Next, the behavior of the equipment measured during functional testing is compared to the predictions of the model; significant differences indicate the presence of one or more faults. Once the faults have been fixed, the model is fine-tuned to match the actual performance observed during the functional tests performed to confirm correct operation. The fine-tuned model is then used as part of a diagnostic tool to monitor performance and detect faults during routine operation. In each case, the model is used to predict the performance that would be expected in the absence of faults. A comparator is used to determine the significance

---

**Peng Xu** is a mechanical engineer and **Philip Haves** is a senior staff scientist at the Lawrence Berkeley National Laboratory, Berkeley, Calif. **Moosung Kim** is a graduate student in the Department of Mechanical Engineering, University of California, Berkeley, Calif.

of any differences between the predicted and measured performance and, hence, the level of confidence that a fault has been detected. A comprehensive review of model-based diagnostics techniques is given by Simami et al. (2003) and a discussion of their application to HVAC is given by Benouarets et al. (1994).

In contrast to other functional test procedures, which emphasize start-up and performance under design conditions, the automated functional tests described here are designed to cover the full range of the system operation. The approach involves the use of both closed loop and open loop tests. Open-loop tests check whether the mechanical system works properly over the full range of operation. Closed-loop tests check the coupled behavior of the mechanical equipment and the controller, identifying problems relating to control sequences and their implementation, including loop tuning. In open-loop tests, controllers are overridden and the mechanical equipment forced to the desired operating points. In closed-loop tests, different operating points are achieved by manipulating the controller setpoint.

There are two aspects of functional tests that can be automated: the exercising of the system under test and the analysis

of the results. Tools that automate only one of these two aspects will be referred to as semi-automated. Automation of each aspect is discussed below.

This paper describes simple open loop tests for mixing boxes, variable-air-volume fan systems, and cooling coil subsystems and reports results of field tests designed to test the models and the data analysis procedures implemented in a prototype automated functional testing tool. Further results are presented by Xu et al. (2004a).

## METHOD

The development of a test procedure for a particular component, subsystem, or system starts with the specification of the faults to be detected. In the work reported here, test procedures were designed with the aim of detecting all the common faults in air-handling units. Table 1 is a list of all the common faults for the mixing box, coil/valve, and supply/return subsystems reported in a survey by Yoshida et al. (1996). The major faults of these three subsystems can be classified into five groups, based on a classification presented in Haves et al. (1996):

**Table 1. Common Faults in HVAC Secondary Systems**

	Mixing Box	Supply/Return Fan	Heating/Cooling Coil & Valve
Group I Fault	Leakage of outside air damper	Range error in variable-frequency drive	Control valve leakage
	Incorrect minimum position of outdoor air damper		Valve or actuator stuck open or partially open
Group II Fault	Outside or exhaust dampers stuck closed or partially closed	Complete failure, e.g., seized, broken belt, power tripped	Valve or actuator stuck closed or partially closed
	Leakage of return air damper	Wrong type of fan	Coil, valve, or pipe blocked
	Return air damper stuck open or partially open	Incorrect rotation direction or wrong fan installed	Filter partially clogged
		Undersized fan	Fouled coil
		Stuck at intermediate speed	Undersized coil
Group III Fault	Damper(s) or actuator(s) stuck	Complete failure, e.g., seized, broken belt, power tripped	Incorrect function of DP sensors
	Actuators fail to respond to changing control signal	VFD or inlet guide vanes fail to respond to changing control signal	Valve or actuator stuck
	Sensor offset/failure	Sensor offset/failure	Actuator fails to respond to changing control signal
Group IV Fault	Hysteresis in actuator(s) or damper linkage(s)	Hysteresis in VFD or inlet guide vanes	Sensor offset/failure
	Damper and actuator mismatch	Variable speed drive malfunction	Hysteresis in actuator or valve linkage
	Excessive nonlinearity		Improper installation of actuator and valve
Group V Fault	Poor loop tuning	Poor loop tuning	Poor valve authority
	Software error	Software error	Poor loop tuning
	Incorrect control signal	Incorrect control signal	Software error
			Incorrect control signal

**Table 2. Open-Loop Test Sequence for Mixing Boxes**

Step Number	Demanded Damper Position (%)	Fault to be Detected
1	0	Outside air damper leakage
2	10	Damper/actuator mismatch
3	50	Nonlinearity
4	90	Damper /actuator mismatch
5	100	Recirculation air damper leakage
6	50	Hysteresis

- I. Faults detectable at minimum control signal, e.g., leakage
- II. Faults detectable at maximum control signal, e.g., coil fouling, undersized equipment
- III. Faults detectable because the target component fails to respond to change in control signals, e.g., stuck actuator, bad communication between controller and actuator
- IV. Faults occurring across the operating range and detectable from the response of the target components in the middle range of the operation, e.g., hysteresis, sensor offset
- V. Faults related to control, e.g., poorly tuned controller, incorrectly implemented sequence of operations

The faults are grouped in this way because it is relatively easy to determine which type of fault exists based on a simple analysis of the performance data generated during the tests. For example, if the system fails to turn off completely, there is a Group I fault. If the system fails to achieve the expected capacity, there is a Group II fault. If the system fails to respond at all to the active control signal, there is a Group III fault. If the system fails an open loop test in the middle of the operating range, there is a Group IV fault. If the system passes the open loop tests but fails the closed loop tests, there is a Group V fault. Within each group, a more detailed rule-based fault diagnosis method can be then used to further diagnose the exact fault.

### Test Procedures

The test procedures are designed to detect all the faults by exercising the systems over their full range of operation. Although the functional tests presented here for the mixing box, fan, and coils differ in detail, the general ideas are the same. Faults in Group I, II, and III can be detected by analyzing the performance at each end of the operating range. To test for mismatch between the range of an actuator and a valve or damper, the control signal is changed by a small amount at each end of the range. Mismatch is typically caused by incorrect adjustment of the linkage between the actuator and the valve or damper, though occasionally it is caused by the installation of an actuator with too small a travel. Hysteresis is detected by approaching a selected point in the middle of the

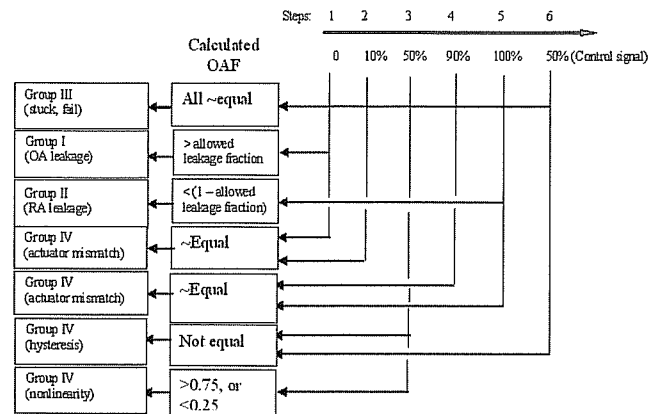


**Figure 1** Fault diagnosis diagram for the mixing box test.

operating range from both directions; a significant difference in the output of the system indicates hysteresis. If the models used to analyze the results of the test are steady-state models, only measurements taken when the system is close to steady state can be used. At each step, a steady-state detector verifies that the system is in steady state before the data are recorded and the test moves on to the next step.

Table 2 lists the minimum sequence of operating points for an open-loop mixing box test. The control points required for the test are:

### Measured Points

- Return air temperature ( $T_{ret}$ )
- Outside air temperature ( $T_{out}$ )
- Mixed air temperature ( $T_{mix}$ ), if present and considered reliable
- Supply air temperature ( $T_{sup}$ ), used when mixed air temperature sensor is missing or unreliable; subtract assumed/calculated temperature rise across supply fan to estimate mixed air temperature
- Damper position (control signal)

### Calculated Point

$$OAF = \frac{T_{mix} - T_{ret}}{T_{out} - T_{ret}} \quad (1)$$

Figure 1 illustrates the identification of the different fault groups from the measured outside air fraction (OAF). The system is exercised by means of a series of step tests in which the damper position is increased from 0% to 100% and then decreased to 50%. At each step, the outside air fraction is calculated in order to identify the presence of one or more faults. The identification can either be performed by a direct comparison of the measured outside air fraction at different operating points or by comparing the deviations of the

**Table 3. Open-Loop Test Sequence for Heating and Cooling Coils**

Step Number	Demanded Valve Position (%)	Fractional Airflow (%)	Fault to be Detected
1	0	Minimum	Leakage
2	10	Minimum	Valve/actuator mismatch
3	25	100	Nonlinearity
4	100	100	Capacity
5	100	Minimum	Valve/actuator mismatch
6	90	Minimum	Valve/actuator mismatch
7	25	100	Hysteresis

**Table 4. Open-Loop Test Sequence for VAV Fan Subsystem**

Step Number	Demanded Fan Speed/Capacity (%)	Terminal Box Damper Openings	Fault to be Detected
1	0	Minimum	Range error in VFD/inlet guide vane, sensor offset
2	50	Minimum	Hysteresis in VFD/inlet guide vane
3	90	Maximum	Range error in VFD
4	100	Maximum	Capacity
5	50	Minimum	Hysteresis in VFD/inlet guide vane

measured outside air fractions from those predicted by a reference model (see below).

Table 3 shows the minimum sequence of operating points for an open-loop heating or cooling coil test. Minimum airflow is used to detect control valve leakage since this maximizes the air-side temperature change across the coil. Minimum airflow also minimizes the temperature rise across the supply fan and the corresponding uncertainty in that temperature rise, minimizing the error in the inference of off-coil temperature from the measurement of supply air temperature (see below). Minimum airflow is also used for Steps 2, 5, and 6 for the same reason. A control signal value of 25% is used for Steps 3 and 7 since control valves are typically oversized, with the result that the temperature rise or drop across the air-side of the coil changes more rapidly in the first half of the operating range than in the second half. It is then easier to characterize any nonlinearity and hysteresis at a control signal value that is significantly less than 50%. In situations in which it is not possible to vary the airflow rate or there is pressure of time, the test can be simplified by using the same airflow rate for all steps.

Table 4 shows the minimum sequence of operating points for an open-loop test of a VAV fan subsystem consisting of either a supply fan and the associated supply system flow resistances or a return fan and the associated return system flow resistances. The supply and return fans should be tested in parallel to limit the variation in building pressure.

After passing the open loop tests, the system is then subjected to the closed loop tests. The procedures for the closed loop tests are similar to those for the open loop tests, except that it is the control setpoints that are changed instead

of the control signal. The setpoints are increased in steps from their minimum to their maximum allowed values. As in the open loop tests, a steady-state detector analyzes the trended data to determine whether the system is in steady state before moving on to the next step.

The test procedures for the mixing box, fan, and coil are described below. The measurement points required for the tests are listed, and rules for faults diagnosis are presented also. The diagnostic procedure for mixing boxes is illustrated in Figure 1, as an example. The diagnostic procedures for fan and coil subsystems are essentially similar.

## Execution

For each functional test, there are a number of conditions that must be satisfied before the test can be conducted. For example, for the mixing box test, the fans must be running and the difference between the outside air temperature and the return air temperature must exceed a minimum value (ideally ~20°F [11°C]) to avoid the estimation of the outside air fraction being dominated by sensor errors. If the supply air temperature, corrected for the temperature rise across the fan, is used as a proxy for the mixed air temperature, the heating and cooling coil valves must be closed. Since these valves may leak, it is better to turn off the circulation pumps as well. These and other checks need to be incorporated in a fully automated tool. A test signal generator was developed to facilitate the automated functional tests. The tool automatically generates the test sequence and signal described above. There is a trend module to record the data and a steady-state detector module to determine whether the system is in steady state. The

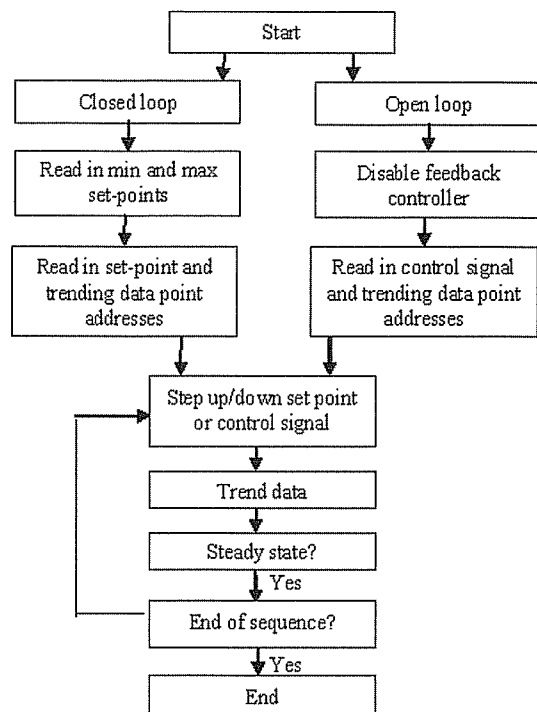


**Figure 2** Automated test signal generator.

step tests will move on to the next step after the system reaches steady state. Figure 2 is a flow chart of the active test tool. On start-up, the tool requires the user to choose between the closed loop test and the open loop test. If the open loop test is selected, the feedback control loop is then disabled.

If closed loop is selected, the maximum and minimum values of the setpoint are needed as inputs. After that, the program requires the user to input the addresses or names of the control and sensor points. The step test generator will then override the control signal value automatically, based on predefined sequence, as described above. The new value is then uploaded into the controller. The trended data are analyzed in real time to determine whether the system is in steady state. When the system reaches steady state, the tool will move to the next step, until the end of the test sequence. The software structure is generic, with only the data transfer between control system and the software being vendor-specific.

## AUTOMATED ANALYSIS

In the approach adopted here, the analysis of the test results is divided into two stages: fault detection and fault diagnosis. Fault detection is performed by comparing the measured behavior to that predicted by a model configured using design information and manufacturers' data. The models may be based on first principles or may be empirical or may be a hybrid, depending on the component and the nature of the information that specifies expected performance

that is available during commissioning. Models of the three air-handling unit subsystems discussed above are described below. Fault diagnosis is performed by using rules to analyze the variation across the operating range of the deviation between the expected and measured performance. The fault diagnosis method is not addressed further in this paper.

## DESCRIPTION OF MODELS AND THEIR DATA REQUIREMENTS

The field tests are focused on three component models in the model library described by Xu and Haves (2004): the mixing box, the VAV fan subsystem, and the cooling coil subsystem. A brief overview of these models is presented here; more detailed information is given in Xu and Haves (2004a). Table 5 list the inputs, outputs, and parameters of the models. In general, measured values of all the inputs to a model are required to drive the model, and a measured value of at least one of the model outputs is required in order to compare the performance of the real system to that predicted by the model. One issue in modeling for fault detection is that some degree of imperfect operation may be tolerated in practice (e.g., leakage of valves or dampers) and so must be included in models that ostensibly represent correct operation.

### Mixing Box

Prediction of the mixed air temperature and humidity in an air-handling unit involves estimating the outside and return air fractions and then performing heat and moisture balances on the mixed airstream. Prediction of the airflow fractions from first principles is impractical because (1) the return air and mixing plenum pressures change with fan speed and (2) it is difficult to estimate airflow resistances in mixing boxes. This said, the behavior in the middle of the operating range is relatively unimportant compared to the behavior at each end of the operating range. An empirical approach to modeling the airflow fractions has therefore been adopted.

At the commissioning stage, when only design information is available, the model describes the range of acceptable behavior. A 3:1 gain variation is used by default; when the damper position is 50%, the permitted upper limit of the outside air fraction is 75%, and the lower limit is 25%. The maximum acceptable deviations from 0% and 100% outside air fraction at each end of the operating range, which are determined by the leakage in the dampers, should be specified by the designer, based on the performance required and manufacturer's data. Note that leakage can arise from imperfections in the dampers themselves, from incorrect installation in the duct or from a mismatch between the ranges of operation of the damper and its actuator. Once the mixing box has been commissioned, the results of the functional test can be used to fit a polynomial to the measured variation of the outside air fraction with the control signal to the damper actuator. The mixed air temperature predicted by the model can be used as an estimate of the entering air temperature for the coils downstream.

**Table 5. Model Inputs, Outputs, and Parameters**

	Inputs	Outputs	Parameters
Mixing box	<ul style="list-style-type: none"> <li>control signal to damper actuators</li> <li>outside air temperature</li> <li>return air temperature</li> <li>outside air humidity</li> <li>return air humidity</li> </ul>	<ul style="list-style-type: none"> <li>mixed air temperature</li> <li>mixed air humidity</li> </ul> <p>Since mixed air temperature is often not measured and mixing is often incomplete anyway, supply air temperature (corrected for temperature rise across the supply fan) is often used as a proxy for mixed air temperature when the coils are inactive.</p>	<ul style="list-style-type: none"> <li>installed return damper leakage (0-1)</li> <li>installed outside air damper leakage (0-1)</li> <li>outside air fraction when damper position is 0.5</li> <li>polynomial coefficients for curve fit of outside air fraction as a function of damper position</li> </ul>
VAV fan subsystem	<ul style="list-style-type: none"> <li>fan speed (assumes variable speed drive)</li> <li>volumetric air flow rate</li> </ul>	<ul style="list-style-type: none"> <li>supply fan: supply duct static pressure</li> <li>return fan: room pressure (may be assumed to be <math>\sim 0.1 \text{ inH}_2\text{O}</math> if not measured)</li> <li>fan pressure rise</li> <li>fan power</li> </ul>	<ul style="list-style-type: none"> <li>fan head curve constants</li> <li>resistance characteristic constants</li> <li>fan efficiency curve constant</li> <li>fraction of motor heat loss entering airstream</li> <li>pressure-fan speed constant</li> <li>fan efficiency</li> <li>maximum fan efficiency</li> <li>motor efficiency</li> </ul>
Coil/valve subsystem	<ul style="list-style-type: none"> <li>control signal to valve actuator</li> <li>water inlet temperature</li> <li>air inlet temperature</li> <li>air inlet humidity</li> </ul>	<ul style="list-style-type: none"> <li>leaving air temperature</li> <li>leaving water temperature</li> <li>leaving air humidity</li> </ul>	<ul style="list-style-type: none"> <li>external heat exchange area</li> <li>internal heat exchange area</li> <li>heat exchange constant for external surface</li> <li>heat exchange constant for internal surface</li> <li>valve authority</li> <li>valve leakage parameter</li> <li>mass flow rate for open valve</li> <li>mass flow rate for closed valve</li> <li>inherent valve resistance ratio (valve resistance divided by valve resistance at full open)</li> </ul>

## VAV Fan System

The model treats VAV systems that have fans with variable speed drives. Fan performance is modeled by using the fan similarity laws to normalize the volumetric flow rate,  $V$ , pressure rise,  $\Delta p_{fan}$ , and power,  $P$ , in terms of the rotation speed,  $n_{fan}$ . The model assumes that the relationship between fan pressure rise and volumetric flow rate over the limited range of normalized flow used in normal operation can be approximated using a constant term and a squared term. The constant term is the pressure rise extrapolated to zero flow rate, which is proportional to the square of the rotation speed, and the squared term corresponds to the pressure drop inside the fan. The model is written in terms of total pressure (i.e., static pressure plus velocity pressure) since energy losses are directly related to changes in total pressure. The pressure rise across the fan is then:

$$\Delta p_{fan} = k_{fan} n_{fan}^2 - C_{fan} V^2 \quad (2)$$

where  $k_{fan}$  and  $C_{fan}$  are empirical constants that will be determined initially from manufacturer's head curve data or from field measurements of flow rate, pressure rise, and rotation speed.

The pressure rise across the fan is balanced by the system pressure drop, which consists of the pressure drop in the other air-handling unit (AHU) components and in the distribution system components. The pressure drop,  $\Delta p_{sys}$ , can be represented by three terms. For the supply fan subsystem, the first term is the total pressure in the supply duct at the position of the sensor used to control the fan speed,  $p_{stat}$ . The second term is the pressure drop across the filter,  $\Delta p_{fil}$ , which is usually measured by a gauge that is read manually. The third term represents the pressure drop through the AHU (except the filter) and the distribution system components upstream of the pressure sensor,  $C_{sys} V^2$ .  $C_{sys}$  is not exactly constant, but varies slightly depending on the relative flow rates in different branches of the duct system. The main components of  $C_{sys}$  are the flow resistances of the coils and sound attenuators, which can be obtained from manufacturers' data. The total pressure at the static pressure sensor is the sum of the static pressure and the velocity pressure ( $\rho V^2/2A^2$ ), where  $\rho$  is the density of air and  $A$  is the cross-sectional area of the duct at the location of the sensor.

$$\Delta p_{sys} = p_{stat} + \Delta p_{fil} + (C_{sys} + \rho/2A^2) V^2 \quad (3)$$

For the return fan subsystem,  $p_{stat}$  is the measured or assumed pressure in the occupied space and appears as a negative term in Equation 3, since a positive pressure in the space reduces the fan pressure rise required. The correction for the velocity pressure in the room is very small and can be ignored.

$$\Delta p_{sys} = -p_{stat} + C_{sys} V^2 \quad (4)$$

Combining the equations for the pressure rise across the fan (2) and the system pressure drop (3) yields:

$$p_{stat} = k_{fan} n_{fan}^2 - (C_{fan} + C_{sys} + \rho/2A^2) V^2 - \Delta p_{fil}, \quad (5)$$

which is used to predict the measured static pressure in the duct (or the pressure in the space) from the fan speed and the airflow rate. If the airflow rate is not measured but there is a measurement of fan pressure rise, the airflow rate can be estimated using Equation 2. A significant difference between the predicted and measured values of the static pressure in the supply duct or the occupied space indicates a fault but does not indicate whether it is in the fan or the distribution system.

If any three of the four measurements relating to the fan, i.e., rotation speed, airflow rate, pressure rise, or fan power,  $P$ , were known, it is possible to determine if there is a fault in the fan using Equation 2 and/or Equation 6:

$$P = V \Delta p_{fan} / \eta, \quad (6)$$

where the combined efficiency of the motor and fan,  $\eta$ , is determined from catalog data or one time measurement. The efficiency can be assumed to be constant over the range of operation or it can be approximated by a quadratic relationship in the normalized flow rate,  $V/n$ , about the maximum value,  $\eta_{max}$ :

$$\eta = \eta_{max} - E(V/n - V_{max}/n)^2 \quad (7)$$

where  $E$  is a constant that is calculated from the manufacturer's data.

If there is no fault in the fan, a fault in the distribution system can be detected using Equation 3, supplemented by Equation 2 and/or Equation 6 as necessary, depending on which variables are measured. One advantage of using SPARK for this problem is that it automatically selects the required equations and the appropriate inverses, depending on which variables are specified as inputs.

Finally, when assessing the thermal performance of the mixing box and coils, it is useful to be able to use the measurement of supply air temperature as a proxy for the mixed air temperature or the off-coil air temperature. Depending on the configuration of the air-handling unit, this may require correcting for the temperature rise,  $\Delta T$ , across the fan, which can be estimated from the pressure rise and the efficiency:

$$\Delta T = \Delta p_{fan} / \eta \rho c_p \quad (8)$$

where  $c_p$  is the specific heat of air at constant pressure.

## Cooling Coil and Control Valve

Cooling coils typically have four or more rows and are essentially counterflow devices. They may provide dehumidification as well as sensible cooling and the surface in contact with the air may then be partially or completely wet. Cooling coils are controlled by varying the flow rate of water through the coil. Coils in VAV systems also experience variable air flow rate. The challenges in cooling coil modeling are to treat the variation in surface thermal resistance with flow rate and to treat partially wet operation.

The most common fault to be detected in cooling coils is fouling of the heat exchange surface, either on the air or the water side. In order to detect fouling when it occurs, it is only necessary to model full-load operation. However, in order to be able to predict the loss of capacity at peak load before it occurs, it is necessary to model part-load operation as well.

In the cooling coil model developed in the work described here, the coil is divided into a number of discrete sections along the direction of fluid flow. In each section, heat and mass balance equations are established for each fluid, together with rate equations describing the heat and mass transfer. If the dew-point temperature of the air is lower than the metal surface temperature, that section of the coil is treated as dry. If not, the water condensation rate is assumed to be proportional to the difference between the humidity ratio of the bulk airstream and the humidity ratio of saturated air at the temperature of the coil metal surface. The coefficient of proportionality is determined by assuming the value of the Lewis number is unity. For simplicity, the heat transfer coefficients for air and water are assumed to vary as the 0.8 power of the fluid flow rate over the whole operating range, and the air-side heat transfer coefficient is assumed to be independent of whether the surface is wet or dry.

The sections that make up the coil are linked together by associating the fluid inlet conditions of one section with the outlet conditions for the adjacent upstream section. SPARK then solves the resulting set of coupled equations. The model is more robust than some other cooling coil models and the greater computational burden associated with the discretization is not expected to be a problem in on-line fault detection applications.

The most common faults associated with control valves are leakage, stuck valve/actuator, and actuator/valve range mismatch. In order to detect these faults, it is more important to model the valve behavior at each end of the operation than in the middle. However, as noted above, it is desirable to be able to predict the part-load performance of coils in order to anticipate loss of peak capacity before it occurs. Since the water flow rate through a coil is not generally measured in HVAC systems, it is necessary to treat the behavior of the control valve at intermediate flow rates by modeling its inherent and installed characteristics in order to predict the water flow rate through the coil.

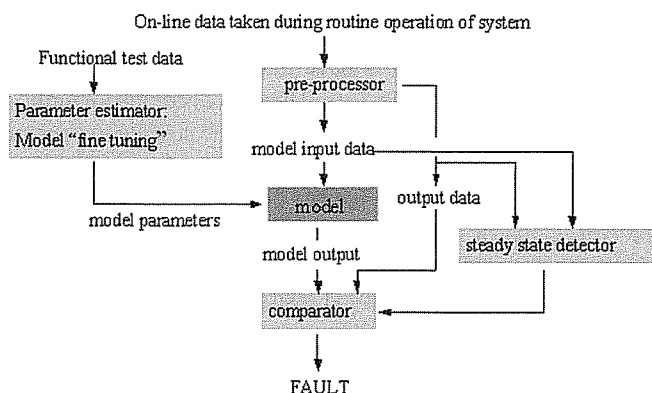


**Figure 3** Data flow of the model-based component-level FDD method.

The water flow rate is a function of the valve position, the flow rate through the valve when fully open, and the leakage. The flow characteristic is assumed to be parabolic, which is an adequate and convenient approximation to the modified equal percentage characteristic used in most control valves intended for this application. More detailed information regarding the coil and valve models is given in Xu and Haves (2004a).

Two approaches to the calibration of the coil model from manufacturer's data are used. If performance data are available at more than one combination of fluid flow rates and/or sensible to latent ratio, these data are used to estimate the values of the coefficients in the air-side and water-side conductance correlations. If only a single rating point is available, it is used to estimate the combined conductance, and the separate values of the air-side and water-side conductance coefficients are then estimated using the typical values of the ratios of these coefficients for different types of coils given by Holmes (1982).

## IMPLEMENTATION OF THE MODEL-BASED ANALYSIS

A toolbox of software routines that support the model-based fault detection methods has also been developed. The toolbox includes a preprocessor, a steady state detector, a comparator, and a framework to support the data flow and analysis. The use of these routines is illustrated in Figure 3 and documented by Xu et al. (2004c).

## FIELD TEST SITES

Test results from two sites are presented. The full test procedure for each subsystem consisted of the following steps: (1) collect HVAC system design information; (2) configure the model using design information and catalog data; (3) perform an active functional test to exercise the subsystem of interest over its operating range; (4) compare the predicted and measured performance and determine whether any significant differences are due to real faults in the subsystem or deficiencies

in the model; (5) calibrate the model using fault-free performance data; (6) determine whether the model can produce an adequate fit to the measured data. The control signal changes were introduced manually, so the results provide a demonstration of the automated analysis method but not the automated execution method.

## Test Site A

Test Site A is a real building that is operated as an experimental facility. The HVAC system consists of three variable-air-volume (VAV) air-handling units: a matched pair that serve test rooms and a single unit that serves the occupied spaces. The data used here are from one of the matched pair (AHU\_A) and are expected to be representative of the measurements that would be obtained from functional tests on a well-controlled system. The measurements were made by the facility staff under carefully controlled conditions using well-established procedures. One advantage of this facility is that the sensors are regularly calibrated, so that sensor error is unlikely to confound the experimental results. Another advantage of an experimental facility is that faults can be introduced into the HVAC system for testing purposes. The data presented here are the results of two sets of step tests on the mixing box, one set with it operating correctly and one with a fault that had been introduced deliberately. All the step tests were open loop tests that were conducted by overriding the feedback controller and adjusting the output signal from minimum to maximum, and then from maximum to minimum, in a predetermined series of steps. Relatively large numbers of steps were employed in order to determine which particular steps provide the most useful information. As discussed above, it is anticipated that the tests used in practice will use fewer steps.

## Test Site B

Test Site B is a 100,000 ft<sup>2</sup> commercial office building built in the 1960s and located in downtown San Francisco. The building has two chillers and one main air-handling unit. The air-handling unit consists of a mixing box, a cooling coil, a supply fan, and a return fan. The return fan is controlled so as to maintain a fixed pressure in the building. There is no heating coil in the air-handling unit and the heating load is satisfied by reheat coils in the terminal boxes in the exterior zones of each floor. Approximately half of the floors of the building are equipped with constant-flow terminal boxes and the other half are equipped with variable-air-volume terminal boxes. The supply and return airflow rates are not measured, but there are measurements of fan pressure rise and power consumption for each fan.

Functional tests were performed on the supply fan and the return fan. The tests were designed to be performed while the building was occupied, which required the tests to be relatively short and have limited impact on indoor thermal comfort. Open-loop functional testing was conducted by overriding the



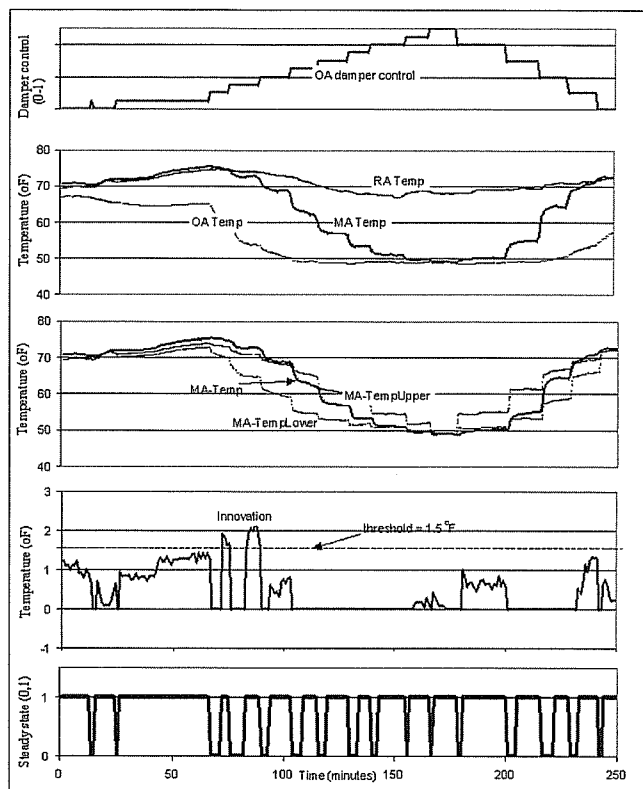


**Figure 4** Test results for mixing box with no artificial fault.

controller and forcing the requested fan speed to the desired values.

## FIELD TEST RESULTS

### Mixing Box

The results for the test at Test Site A on the mixing box with no deliberate fault are shown in Figure 4. The requested position of the damper actuators and the measurements of the outside, return, and mixed air temperatures are shown at the top of the figure. Since there is relatively poor mixing in most mixing boxes, the supply air temperature, corrected for the rise across the supply fan using Equation 8, is used as a proxy for the mixed air temperature. The maximum mixed air temperature is very close to the return air temperature, and the minimum mixed air temperature is very close to the outside air temperature, indicating that leakage is small. In the middle of the figure is a comparison of the measured mixed air temperature and the mixed air temperatures corresponding to the 3:1 gain range that define the limits of acceptable operation, as described above. In the absence of any specific information on acceptable leakage, the values of the acceptable leakage parameters were set to zero. The measured values lie between the permitted upper and lower limits, except when the

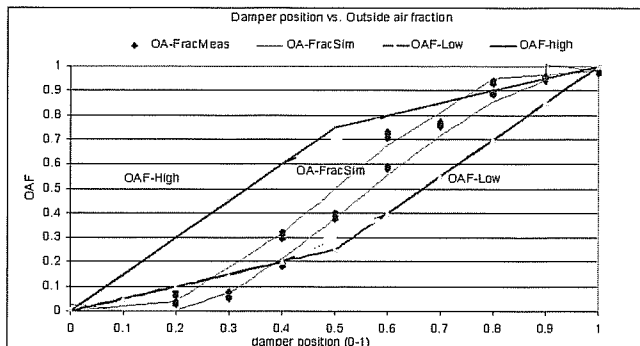


**Figure 5** Mixing box characteristics.

requested position of the damper is ~20%, when the damper fails to open significantly, in part because of hysteresis.

Figure 5 shows a plot of outside air fraction versus damper position for the acceptable limits, the measured values and separate polynomial fits to the ascending and descending measurements, which constitute the model for use in routine operation. The lower part of Figure 4 is a plot of the output of the steady state detector, in which a value of unity indicates steady state, and of the “innovation,” the absolute difference between the measured and acceptable values of the mixed air temperature. The innovation is only meaningful when the system is in steady state and is displayed as zero when the system is not in steady state. The threshold value of 1.5°F allows for sensor errors (which are expected to be small at test site A); there is no need to allow for modeling errors in this case because the mixing box model used for commissioning is prescriptive. The innovation exceeds the threshold when the control signal is ~20% and the outside air damper is opening, indicating a combination of hysteresis and actuator/damper range mismatch. The magnitude of these faults is not large and, for the purposes of illustrating the method, the model fitted to the measurements will be considered to be a model of acceptable operation.

Figure 6 shows the result of using the model fitted to measurements from the correctly operating mixing box to detect faults in a mixing box with an artificially induced fault. In this case, the return air damper had been fixed in the closed position by the facility staff, as if the actuator had failed. The outside and exhaust air dampers were closed in 10% steps and then opened in 20% steps, as shown at the top of the figure. The third plot shows that the measured performance falls significantly outside the permitted range, which is the comparison that would be performed as part of initial commissioning. Lower down is the comparison of the measured performance and the performance simulated by the model fitted to the correct operation data, which is the comparison that would be performed if the functional test were repeated to check performance subsequent to the initial commissioning. At the bottom are the corresponding output of the steady state detector and innovations. The threshold has been increased to 3°F to reflect

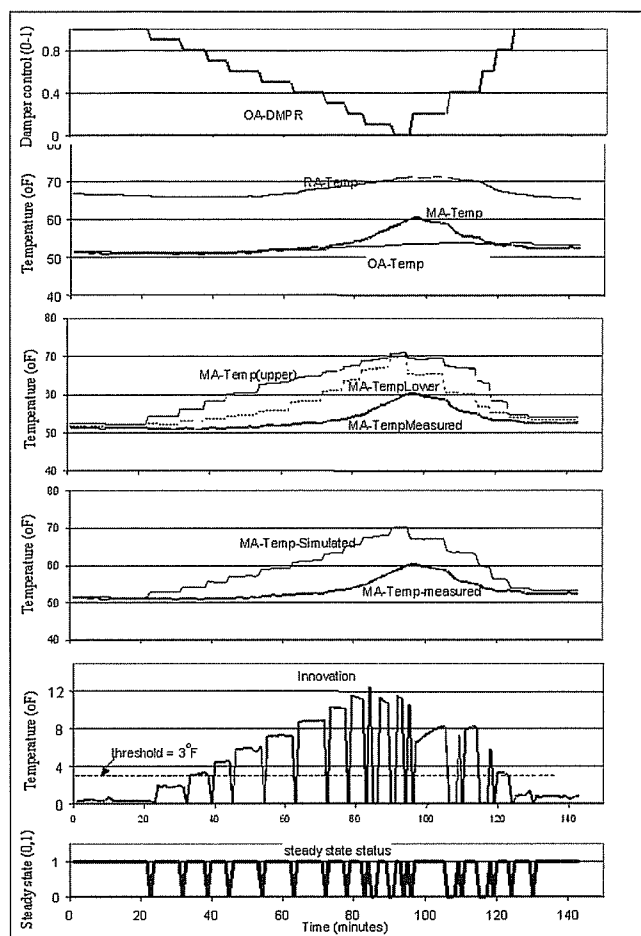


**Figure 6** Test results for mixing box with artificial fault.

the modeling errors that must be considered when the reference model is a fit to performance data. The innovations significantly exceeded the threshold for much of the operating range, indicating the presence of a substantial fault. In both Figure 4 and Figure 6, significant innovations occur at one or more of the control signal values used in the test procedures described in the “Method” section above (0%, 10%, 50%, 90%, 100%), demonstrating that these faults can be detected with the minimal test signal set described.

## Fan Systems

Models of the supply and return fan subsystems at test site B were configured using manufacturers’ data. As can be seen from Figure 7, part of each test was performed in open loop by overriding the requested fan speed signal to the variable frequency drive. The rest of each test was performed in closed loop by reducing the setpoint for the static pressure in the supply duct or in the occupied space. Because the building was occupied at the time of the tests, the tests cover only a limited part of the operating range. The part of the analysis reported here focuses on the fans themselves. Figures 7A and 7C show

the speed and power recorded for each fan during the tests. Since the airflow rate is not measured at this site, it was predicted from the measured pressure rise and power using the manufacturer’s efficiency data and Equations 6 and 7. The pressure rise was then predicted from the calculated flow rate, the rotation speed, and a simple, two-parameter fit to the manufacturer’s head curve, using Equation 1. Figures 7B and 7D show the predicted and measured pressure rise for the two fans. There is good agreement for the return fan but not for the supply fan. After talking with the building operator, it emerged that the supply fan had a problem with slipping belts, which led to the measured pressure rise being significantly lower than expected from the requested rotation speed and the measured power.

## SUMMARY AND CONCLUSIONS

A model-based functional testing methodology has been described and demonstrated using measured data. A systematic procedure for designing active tests has been presented and verified for the case of a mixing box. A software implementation of the model-based analytical procedure detected multiple faults in the mixing box, and a model-based analysis detected a fault in an air-handling unit fan. Ongoing work includes an international effort to extend the model library, including the verification of the ability of the models to represent correct operation of real HVAC equipment, investigation of methods of selecting detection thresholds, and the development of a hybrid approach to fault diagnosis that involves the use of rules to diagnose faults based on the differences between measured behavior and that predicted by a model. The model-based methodology also supports an integrated approach that links design, commissioning, and operations, allowing the actual performance of the building and the HVAC system to be tested against the engineering design intent.

## ACKNOWLEDGMENTS

The authors wish to thank Johnson Controls Inc. for providing measurements made at the Iowa Energy Center. They also gratefully acknowledge the assistance of John House, Dick Kelso, Tim Salsbury, Fred Smothers, and Ted Ludwick. This work was supported by the California Energy Commission PIER Buildings Program and by the Assistant Secretary for Energy Efficiency and Renewable Energy, Office of Building Technology, State and Community Programs, of the U.S. Department of Energy under Contract No. DE-AC03-76SF00098.

## REFERENCES

- Benouarets, M., A.L. Dexter, R.S. Fargus, P. Haves, T.I. Salsbury, and J.A. Wright. 1994. Model-based approaches to fault detection and diagnosis in air-conditioning systems. *Proceedings of System Simulation in Buildings '94, Liège, December*.
- Haves, P., D.R. Jorgensen, T.I. Salsbury, and A.L. Dexter. 1996. Development and testing of a prototype tool for

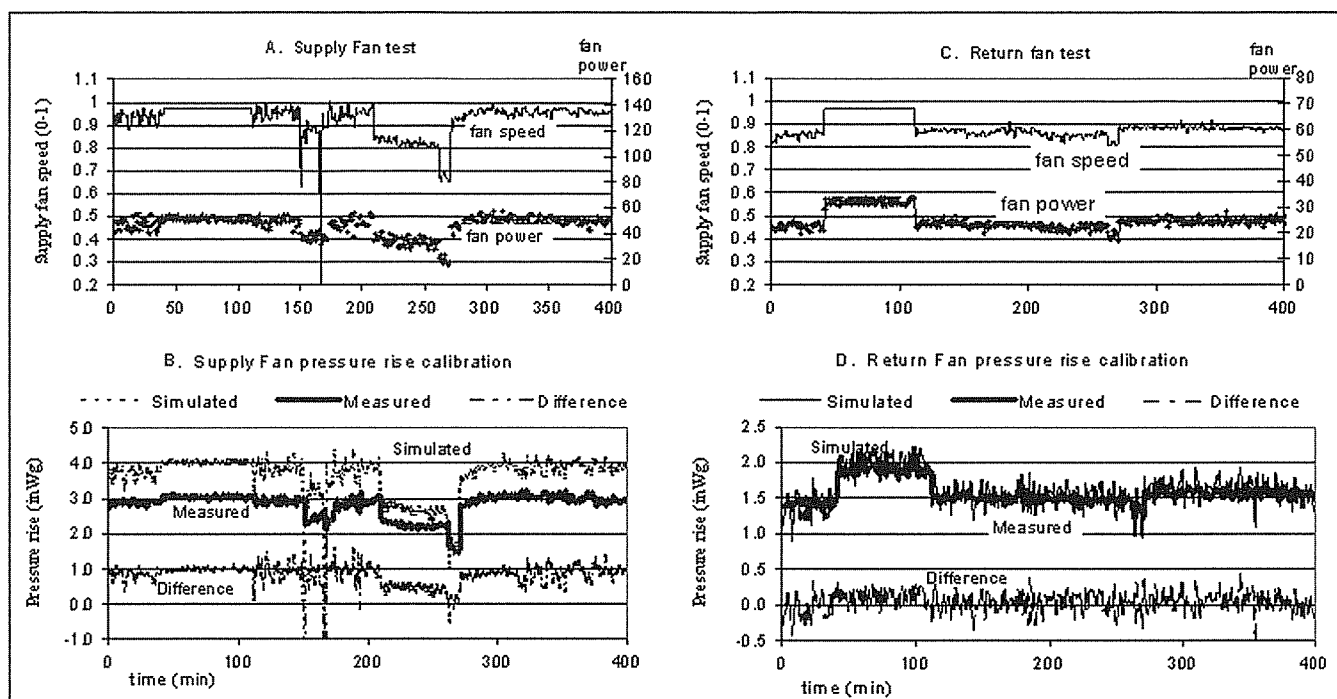


Figure 7 Results of fan tests.

- HVAC control system commissioning. *ASHRAE Transactions* 102(1).
- Haves, P., and S.K. Khalsa. 2000. Model-based performance monitoring: review of diagnostic methods and chiller case study. *Proceedings of ACEEE Summer Study, Asilomar, CA, August*. LBNL-45949.
- Holmes, M.J. 1982. The simulation of heating and cooling coils for performance analysis. *Proceedings of System Simulation in Buildings '82, Liège, Belgium*.
- Hyvärinen, J., and S. Kärki. 1997. IEA Annex 25 Final Report, VTT, Espoo, Finland.
- LBNL. 1999. *Proceedings of Diagnostics for Commercial Buildings: From Research to Practice, San Francisco, CA*. <http://poet.lbl.gov/diagworkshop/proceedings>.
- Ngo, D., and A.L. Dexter. 1998. Automatic commissioning of air-conditioning plant. *Proc. Control '98, UKACC Int Conf, Swansea, Wales, September 1998*, Vol 2, pp 1694-1699. IEE Conf Publication 455.
- Sellers, D., T. Haasl, H. Friedman, M.A. Piette, and N. Bourassa. 2003. Control system design guide and functional testing guide for air handling systems. Public release at NCBC 2003, *Proceedings of the 11th National Conference on Building Commissioning*. May.
- Simani, S., C. Fantuzzi, and R.J. Patton. 2003. *Model-Based Fault Diagnosis in Dynamic Systems Using Identification Techniques*. New York: Springer.
- SPARK. 2004. *Simulation Problem Analyses and Research Kernel*. Lawrence Berkeley National Laboratory and Ayres Sowell Associates, Inc. Berkeley, CA.: Lawrence Berkeley National Laboratory. <http://simulationresearch.lbl.gov>.
- Xu, P., and P. Haves. 2004a. Library of component reference models for fault detection (AHU and chiller). Report to California Energy Commission. Berkeley, CA.: Lawrence Berkeley National Laboratory.
- Xu, P., M. Kim, and P. Haves. 2004b. Tests of component-level model-based fault detection methods using field data. Report to California Energy Commission. Berkeley, CA.: Lawrence Berkeley National Laboratory.
- Xu, P., M. Kim, and P. Haves. 2004c. Software toolbox for component-level model-based fault detection methods. Report to California Energy Commission. Berkeley, CA.: Lawrence Berkeley National Laboratory.
- Yoshida, H., T. Iwami, H. Yuzawa, and M. Suzuki. 1996. Typical faults of air-conditioning systems and fault detection by ARX model and extended Kalman filter. *ASHRAE Transactions* 102(1).

## DISCUSSION

**Bruce Billedeaux, Engineer, GE Automation Services, Portage, Mich.:** Is there a research activity to standardize point labels to reduce the time and cost to set up the data collection from the EMCS?

**Peng Xu:** I think this is a very important issue that needs to be resolved sooner rather than later. However, there is no such research that I am aware of. I think this question should be partially addressed by the collaboration of major control vendors or by ASHRAE. There are several related research activities in Industry Foundation Class (IFC) to translate the control algorithm and eventually point labels between software.

